

Article type : Research Article

# Synthesis and *in vitro* anticancer activities of selenium *N*-heterocyclic carbene compounds

Sheng Huang<sup>a,1</sup>, Xinyu Sheng<sup>a,1</sup>, Mianli Bian<sup>a</sup>, Zhibin Yang<sup>a</sup>, Yunlong Lu<sup>a\*</sup> and Wukun Liu<sup>a\*</sup>

<sup>a</sup>Jiangsu Collaborative Innovation Center of Chinese Medicinal Resources Industrialization, School of Pharmacy, School of Medicine & Holistic Integrative Medicine, Nanjing University of Chinese Medicine, Nanjing, 210023, China

## Corresponding Author

\* Corresponding author. Nanjing University of Chinese Medicine, Nanjing, 210023, China

E-mail: yunlonglu12@njucm.edu.cn (Y. L.);

liuwukun0000@hotmail.com, liuwukun0000@njucm.edu.cn (W. L.)

Tel: +86-25-85811357

## Author Contributions

<sup>1</sup> Sheng Huang and Xinyu Sheng contributed equally to this work.

## Abstract

Fourteen novel selenium *N*-heterocyclic carbene (Se-NHC) compounds derived from 4,5-diarylimidazole were designed, synthesized, and evaluated as antiproliferative agents. Most of

This article has been accepted for publication and undergone full peer review but has not been through the copyediting, typesetting, pagination and proofreading process, which may lead to differences between this version and the [Version of Record](#). Please cite this article as [doi: 10.1111/CBDD.13900](https://doi.org/10.1111/CBDD.13900)

This article is protected by copyright. All rights reserved

---

them were more effective towards A2780 ovarian cancer cells than HepG2 hepatocellular carcinoma (HCC) cells. Among them, the most active compound **2b** was about 4-fold more active than the positive control ebselen against A2780 cells. In addition, this compound displayed 2-fold higher cytotoxicity to A2780 cells than to IOSE80 normal ovarian epithelial cells. Further studies revealed that **2b** could induce reactive oxygen species (ROS) production, damage mitochondrial membrane potential (MMP), block the cells in the G0/G1 phase, and finally promote A2780 cell apoptosis.

**Keywords:** *N*-heterocyclic carbene; selenium compounds; ovarian cancer; antitumor; apoptosis

## 1. Introduction

Cancer is one of the diseases with the highest mortality rate in the world. Among them, ovarian cancer is the main cause of death from all gynecological tumors, and chemotherapy is the main method for the treatment of metastatic ovarian cancer (Kala et al., 2014). However, commonly used chemotherapeutic drugs are often limited in clinic due to highly non-specific cytotoxicity and adverse side effects. Meanwhile, intrinsic and acquired drug resistance is also one of the clinical disadvantages of chemotherapeutics (Siegel, Naishadham, & Jemal, 2013). Therefore, the development of new chemotherapeutic drugs is urgent (Banerjee & Kaye, 2013).

Selenium (Se), as an essential micronutrient, plays a significant role in human health (Hosnedlova et al., 2017; Ibrahim, Kerkadi, & Agouni, 2019). In recent years, researchers focused on the potential therapeutic effects of Se in cancer treatment (An, Wang, et al., 2018). Among them, more and more organoselenium derivatives were developed and studied for their lower toxicity compared to inorganic Se compounds (Reich & Hondal, 2016). Several organoselenium compounds, including ebselen (**Se1**), ethaselen (**Se2**), and Se *N*-heterocyclic carbene (NHC) compounds (**Se3-6**) (**Figure 1**) have been shown to inhibit cancer cell growth *in vitro* and *in vivo* (Engman et al., 1997; Kamal et al., 2019; Lai et al., 2018; Nguyen et al., 2011; Wang et al., 2012; Yang et al., 2009; Zeng, Deng, Sang, Zhao, & Chen, 2018). It was also reported that they have synergistic effects in combination with chemotherapy drugs (Ip, Lisk, & Ganther, 1998; Z. Li et al., 2009). Therefore, organoselenium compounds with different scaffolds have been used as chemotherapeutic agents attributed to their significant anticancer bioactivity (Sanmartin, Plano, &

Palop, 2008).

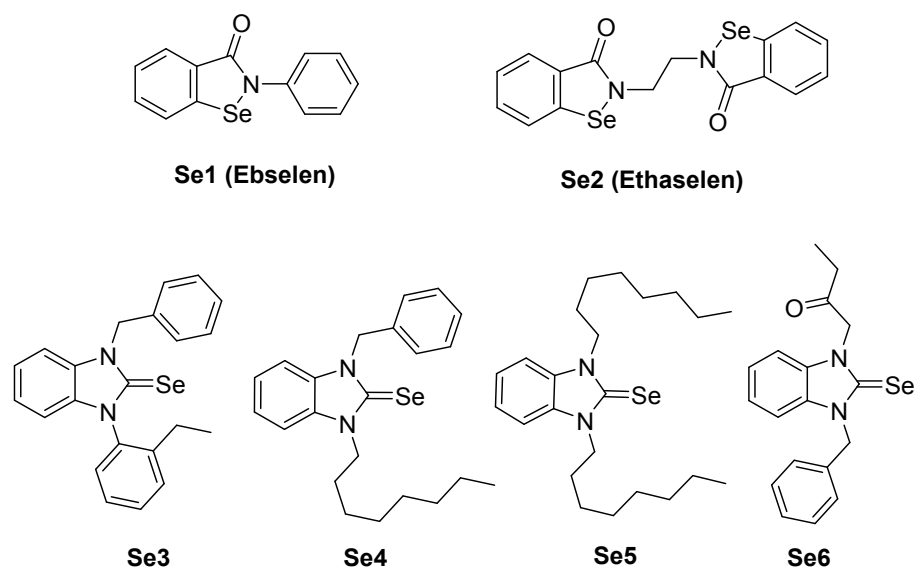


**Fig 1.** The structure of compounds **Se1-Se6**.

NHC was widely used in organic or inorganic chemistry for drug design. As  $\sigma$ -donor or  $\pi$ -acceptor, NHC could easily combine with some metal elements to form stable and biologically active complexes (Garcia-Garcia, Martinez, Sanjuan, Fernandez-Rodriguez, & Sanz, 2011; Gautier & Cisnetti, 2012; Liu & Gust, 2013; Mercs & Albrecht, 2010; Teyssot et al., 2009). Different transition metals including gold (Casini, Sun, & Ott, 2018; Hickey et al., 2008; Liu, Bendsdorf, & Proetto, 2011, 2012; Long et al., 2020; Meyer et al., 2014; Zou, Lum, Chui, & Che, 2013), silver (Liu, Bendsdorf, Hagenbach, et al., 2011), iridium (Gothe, Marzo, Messori, & Metzler-Nolte, 2015; Y. Li et al., 2015; C. Yang et al., 2016), platinum (Harlepp et al., 2019; Rothmund et al., 2020; Tham, Babak, & Ang, 2020) and rhodium (Fan, Bian, Hu, & Liu, 2019) have been designed as metal-based NHC complexes for chemotherapy, and many of them exhibited highly effective anticancer activities both *in vivo* and *in vitro*.

In our previous work, gold(I) and silver(I) NHC complexes derived from 4,5-diarylimidazole showed high inhibitory effects in MCF-7 and MDA-MB 231 breast cancer as well as HT-29 colon cancer cells (Liu, Bendsdorf, Hagenbach, et al., 2011; Liu, Bendsdorf, & Proetto, 2011; Liu et al., 2012). Preliminary structure activity relationships

---

(SAR) study demonstrated that the -F and -OMe groups at the *para*-position of aromatic rings increased the bioactivity of gold(I) NHC complexes in cancer cells. The substituents at the nitrogen atoms, the oxidation state of the metal, and the anionic counterion on these complexes also played significant roles in regulating the bioactivity of them.

Recently, we found that both iodo (1,3-diethyl-4,5-bis(4-methoxyphenyl)imidazole-2-ylidene) gold(I) complex and chloride ( $\eta^2,\eta^2$ -cycloocta-1,5-diene) (4,5-bis(4-fluorophenyl)-1,3-diethylimidazol-2-ylidene) rhodium(I) complex showed strong antiproliferative activity against hepatocellular carcinoma (HCC) cells (Bian et al., 2020; Fan et al., 2019). The mechanism study showed that these NHC complexes can powerfully inhibit the activity of thioredoxin reductase (TrxR). The level of intracellular reactive oxygen species (ROS) was thereby increased, and it damaged the mitochondrial membrane potential (MMP) and induced cell apoptosis. *In vivo* anticancer studies furtherly showed that gold(I) and rhodium(I) NHC complexes can significantly repress tumor growth in a HepG2 xenograft mouse model and ameliorate liver injury caused by CCl<sub>4</sub> in chronic HCC.

In the continuation of our studies, fourteen novel Se-NHC compounds derived from 4,5-diarylimidazole were designed and synthesized, the antitumor activity of these compounds were subsequently evaluated. The 4,5-diarylimidazole salts were used as raw material to obtain Se-NHC compounds and antitumor activities of Se-NHC compounds were tested in HepG2 cells, A2780 cells, and IOSE80 cells by MTT assay. Bioactivity research revealed that the most promising compound **2b** can induce intracellular ROS accumulation and promote apoptosis in A2780 cells.

## 2. Experimental sections

### 2.1. reagents and methods

All reagents used in the synthesis were obtained from Energy Chemical Company (China) without further purification. The deuterated solvent was obtained from Cambridge Isotope Lab Inc. (CIL). Purified TrxR (rat liver) and ct-DNA were obtained from Sigma-Aldrich Co.; JC-1 assay kit was obtained from APExBio (China). Apoptosis kit, ROS detection kit and GSH and GSSG Assay

Kit were obtained from Beyotime (China). DNA content kit was obtained from Key Gen Biotech (Nanjing, China).

HPLC grade solvents and Millipore (> 18.2 MU) double distilled water were used for the preparation of all spectroscopic and biological research solutions. The  $^1\text{H}$  NMR and  $^{13}\text{C}$  NMR spectra were measured by Bruker Avance III HD 500 MHz nuclear magnetic resonance instrument; low resolution mass spectrometry was measured by Agilent 1290-6125 single quadrupole LC/MS spectrometer, ESI ion Source determination; X-ray single crystal structure data collected by BRUKER Smart APEX II CCD; UV/Vis spectra were measured by Shimadzu UV2400 spectrophotometer. Fluorescent microscopy was performed by a Leica DMi8 fluorescence microscope. Flow Cytometry was performed by BD Accuri™ C6 Plus and Beckman Gallios. Microplate detection was performed by Tecan M1000 Pro.

## 2.2. Synthesis of selenium compounds

### 2.2.1. The synthesis of **1a-1n**.

The synthesis of compounds **1a**, **1b**, **1e-1i** and **1k-1n** has been reported previously (Fan et al., 2019). The new analogues **1c**, **1d** and **1j** were prepared by the same route, and their data from  $^1\text{H}$  NMR spectra were listed below.

*3-benzyl-1-ethyl-4,5-bis(4-methoxyphenyl)-1H-imidazol-3-ium bromide 1c*:  $^1\text{H}$  NMR (500 MHz, DMSO)  $\delta$  9.68 (s, 1H, NCHN), 7.40-7.27 (m, 5H, Ar<sub>Ph</sub>H), 7.23-7.06 (m, 4H, Ar<sub>Ph</sub>H), 6.97 (dd,  $J$  = 36.9, 8.6 Hz, 4H, Ar<sub>Ph</sub>H), 5.37 (s, 2H, NCH<sub>2</sub>Ar), 4.12 (q,  $J$  = 7.2 Hz, 2H, NCH<sub>2</sub>CH<sub>3</sub>), 3.76 (d,  $J$  = 10.2 Hz, 6H, OCH<sub>3</sub>), 1.32 (t,  $J$  = 7.2 Hz, 3H, NCH<sub>2</sub>CH<sub>3</sub>).

*1-ethyl-3-(2-methoxyethyl)-4,5-bis(4-methoxyphenyl)-1H-imidazol-3-ium bromide 1d*:  $^1\text{H}$  NMR (500 MHz, CDCl<sub>3</sub>)  $\delta$  10.32 (s, 1H, NCHN), 7.19-7.07 (m, 4H, Ar<sub>Ph</sub>H), 6.89-6.79 (m, 4H, Ar<sub>Ph</sub>H), 4.36 (t,  $J$  = 5.0 Hz, 2H, NCH<sub>2</sub>CH<sub>2</sub>), 4.22 (q,  $J$  = 7.3 Hz, 2H, NCH<sub>2</sub>CH<sub>3</sub>), 3.73 (t,  $J$  = 3.7 Hz, 8H, ArOCH<sub>3</sub>, NCH<sub>2</sub>CH<sub>2</sub>), 3.31 (s, 3H, OCH<sub>3</sub>), 1.43 (t,  $J$  = 7.3 Hz, 3H, NCH<sub>2</sub>CH<sub>3</sub>).

*1-ethyl-4,5-bis(4-fluorophenyl)-3-(3-hydroxypropyl)-1H-imidazol-3-ium bromide 1j*:  $^1\text{H}$  NMR (500 MHz, DMSO)  $\delta$  9.56 (s, 1H, NCHN), 7.51 (ddd,  $J = 8.5, 5.4, 1.5$  Hz, 4H,  $\text{Ar}_{\text{Ph}}\text{H}$ ), 7.33 (td,  $J = 8.8, 2.2$  Hz, 4H,  $\text{Ar}_{\text{Ph}}\text{H}$ ), 4.67 (t,  $J = 5.0$  Hz, 1H, -OH), 4.21 – 4.04 (m, 4H,  $\text{NCH}_2\text{CH}_2\text{CH}_2\text{OH}$ ,  $\text{NCH}_2\text{CH}_3$ ), 3.39 (dd,  $J = 11.1, 5.7$  Hz, 2H,  $\text{NCH}_2\text{CH}_2\text{CH}_2\text{OH}$ ), 1.84-1.75 (m, 2H,  $\text{NCH}_2\text{CH}_2\text{CH}_2\text{OH}$ ), 1.31 (t,  $J = 7.3$  Hz, 3H,  $\text{NCH}_2\text{CH}_3$ ).

### 2.2.2. General procedure for the synthesis of **2a-2m**

**1a-1m** (0.83 mmol, 1 eq) was dissolved in dry THF (10 mL), KOtBu (1.66 mmol, 2 eq), selenium powder (1.24 mmol, 1.5 eq) were added, and the solution was stirred under ice bath for 5 hours. The products (**2a-2m**) were isolated by column chromatography on silica gel (mobile phase: PE/EA, 20:1). The samples were eluted with acetonitrile/ $\text{H}_2\text{O}$  mixture at a constant flow rate. The purity of all Se-NHC compounds is greater than 95% by HPLC analysis (**Figure S5**).

*1,3-diethyl-4,5-bis(4-methoxyphenyl)-imidazole-2-selenone 2a*: white powder (yield 60%).  $^1\text{H}$  NMR (500 MHz,  $\text{CDCl}_3$ )  $\delta$  7.11 (d,  $J = 8.6$  Hz, 4H,  $\text{Ar}_{\text{Ph}}\text{H}$ ), 6.84 (d,  $J = 8.6$  Hz, 4H,  $\text{Ar}_{\text{Ph}}\text{H}$ ), 4.21 (q,  $J = 7.1$  Hz, 4H,  $\text{NCH}_2\text{CH}_3$ ), 3.79 (s, 6H,  $\text{OCH}_3$ ), 1.24 (t,  $J = 6.8$  Hz, 6H,  $\text{NCH}_2\text{CH}_3$ ).  $^{13}\text{C}$  NMR (126 MHz,  $\text{CDCl}_3$ )  $\delta$  159.90 (Se=C), 152.81, 131.86, 120.37, 114.08 ( $\text{Ar}_{\text{Ph}}\text{C}$ ), 129.56 (NC=CN), 55.22 ( $\text{ArOCH}_3$ ), 42.50 ( $\text{NCH}_2\text{CH}_3$ ), 14.44 ( $\text{NCH}_2\text{CH}_3$ ). ESI-MS (+) [m/z]: 416.8 [M+H] $^+$ . Purity: 95.5% (by HPLC). Retention time  $t_{\text{R}} = 15.888$  min.

*1-ethyl-4,5-bis(4-methoxyphenyl)-3-(2,4,6-trimethylbenzyl)-imidazole-2-selenone 2b*: white powder (yield 66.7%).  $^1\text{H}$  NMR (500 MHz,  $\text{CDCl}_3$ )  $\delta$  7.07 (d,  $J = 8.4$  Hz, 2H,  $\text{Ar}_{\text{Ph}}\text{H}$ ), 6.81 (d,  $J = 8.5$  Hz, 2H,  $\text{Ar}_{\text{Ph}}\text{H}$ ), 6.63 - 6.54 (m, 4H,  $\text{Ar}_{\text{Ph}}\text{H}$ ), 6.47 (d,  $J = 8.5$  Hz, 2H,  $\text{Ar}_{\text{Ph}}\text{H}$ ), 5.58 (s, 2H,  $\text{NCH}_2\text{Ar}$ ), 4.27 (d,  $J = 7.1$  Hz, 2H,  $\text{NCH}_2\text{CH}_3$ ), 3.78 (s, 3H,  $\text{ArOCH}_3$ ), 3.71 (s, 3H,  $\text{ArOCH}_3$ ), 2.17 (s, 3H,  $\text{ArCH}_3$ ), 1.94 (s, 6H,  $\text{ArCH}_3$ ), 1.28 - 1.25 (m, 3H,  $\text{NCH}_2\text{CH}_3$ ).  $^{13}\text{C}$  NMR (126 MHz,  $\text{CDCl}_3$ )  $\delta$  155.40 (Se=C), 159.88, 159.51, 136.88, 136.61, 131.82, 131.63, 130.31, 130.25, 129.01, 120.42, 120.24, 113.95, 113.00 ( $\text{Ar}_{\text{Ph}}\text{C}$ ), 130.19 (NC=CN), 55.18, 55.17 ( $\text{ArOCH}_3$ ), 48.16 ( $\text{NCH}_2\text{Ar}$ ), 42.83 ( $\text{NCH}_2\text{CH}_3$ ), 20.67, 20.33 ( $\text{ArCH}_3$ ), 14.46 ( $\text{NCH}_2\text{CH}_3$ ). ESI-MS (+) [m/z]: 441.2 [M-Se] $^+$ . Purity: 99.2% (by HPLC). Retention time  $t_{\text{R}} = 11.764$  min.

*1-benzyl-3-ethyl-4,5-bis(4-methoxyphenyl)-imidazole-2-selenone 2c*: white powder (yield 63.1%). <sup>1</sup>H NMR (500 MHz, CDCl<sub>3</sub>) δ 7.23 (d, *J* = 5.0 Hz, 3H, Ar<sub>Ph</sub>H), 7.16 - 7.05 (m, 4H, Ar<sub>Ph</sub>H), 6.86 (dd, *J* = 8.1, 4.9 Hz, 4H, Ar<sub>Ph</sub>H), 6.72 (d, *J* = 8.5 Hz, 2H, Ar<sub>Ph</sub>H), 5.47 (s, 2H, NCH<sub>2</sub>Ar), 4.29 (q, *J* = 7.0 Hz, 2H, NCH<sub>2</sub>CH<sub>3</sub>), 3.78 (d, *J* = 15.7 Hz, 6H, ArOCH<sub>3</sub>), 1.30 (t, *J* = 7.1 Hz, 3H, NCH<sub>2</sub>CH<sub>3</sub>). <sup>13</sup>C NMR (126 MHz, CDCl<sub>3</sub>) δ 155.20 (Se=C), 159.95, 159.88, 136.65, 132.07, 131.88, 128.31, 127.56, 127.36, 120.25, 120.20, 114.10, 113.81, 130.07(Ar<sub>Ph</sub>C), 129.73 (NC=CN), 55.24, 55.21 (ArOCH<sub>3</sub>), 50.66 (NCH<sub>2</sub>Ar), 42.98 (NCH<sub>2</sub>CH<sub>3</sub>), 14.48 (NCH<sub>2</sub>CH<sub>3</sub>). ESI-MS (+) [*m/z*]: 339.2 [M-Se]<sup>+</sup>, 479.0 [M+H]<sup>+</sup>. Purity: 96.1% (by HPLC). Retention time *t*<sub>R</sub> = 16.628 min.

*1-ethyl-3-(2-methoxyethyl)-4,5-bis(4-methoxyphenyl)-imidazole-2-selenone 2d*: white powder (yield 65%). <sup>1</sup>H NMR (500 MHz, CDCl<sub>3</sub>) δ 7.14 (dd, *J* = 15.6, 8.7 Hz, 4H, Ar<sub>Ph</sub>H), 6.85 (dd, *J* = 8.6, 7.7 Hz, 4H, Ar<sub>Ph</sub>H), 4.33 (t, *J* = 6.0 Hz, 2H, NCH<sub>2</sub>CH<sub>2</sub>), 4.23 (q, *J* = 7.1 Hz, 2H, NCH<sub>2</sub>CH<sub>3</sub>), 3.85 - 3.75 (m, 8H, ArOCH<sub>3</sub>, NCH<sub>2</sub>CH<sub>2</sub>), 3.23 (s, 3H, OCH<sub>3</sub>), 1.26 (t, *J* = 7.1 Hz, 3H, NCH<sub>2</sub>CH<sub>3</sub>). <sup>13</sup>C NMR (126 MHz, CDCl<sub>3</sub>) δ 153.44 (Se=C), 159.91, 159.87, 132.36, 131.93, 120.39, 120.24, 114.08, 113.92 (Ar<sub>Ph</sub>C), 130.53, 129.37 (NC=CN), 69.69 (CH<sub>2</sub>OCH<sub>3</sub>), 58.67 (CH<sub>2</sub>OCH<sub>3</sub>), 55.24, 55.21 (ArOCH<sub>3</sub>), 46.37 (NCH<sub>2</sub>CH<sub>2</sub>), 42.62(NCH<sub>2</sub>CH<sub>3</sub>), 14.41(NCH<sub>2</sub>CH<sub>3</sub>). ESI-MS (+) [*m/z*]: 367.2 [M-Se]<sup>+</sup>, 447.2 [M+H]<sup>+</sup>. Purity: 95.6% (by HPLC). Retention time *t*<sub>R</sub> = 15.870 min.

*4,5-bis(4-bromophenyl)-1,3-diethyl-imidazole-2-selenone 2e*: white powder (yield 86%). <sup>1</sup>H NMR (500 MHz, CDCl<sub>3</sub>) δ 7.54-7.48 (m, 4H, Ar<sub>Ph</sub>H), 7.11-7.02 (m, 4H, Ar<sub>Ph</sub>H), 4.24 (q, *J* = 7.1 Hz, 4H, NCH<sub>2</sub>CH<sub>3</sub>), 1.27 (t, *J* = 7.1 Hz, 6H, NCH<sub>2</sub>CH<sub>3</sub>). <sup>13</sup>C NMR (126 MHz, CDCl<sub>3</sub>) δ 155.12 (Se=C), 132.19, 131.94, 126.84, 123.80 (Ar<sub>Ph</sub>C), 128.89 (NC=CN), 42.72 (NCH<sub>2</sub>CH<sub>3</sub>), 14.39 (NCH<sub>2</sub>CH<sub>3</sub>). ESI-MS (+) [*m/z*]: 433.0 [M-Se]<sup>+</sup>. Purity: 97.1% (by HPLC). Retention time *t*<sub>R</sub> = 11.501 min.

*1,3-diethyl-4,5-bis(4-fluorophenyl)-imidazole-2-selenone 2f*: white powder (yield 56.2%). <sup>1</sup>H NMR (500 MHz, CDCl<sub>3</sub>) δ 7.22-7.16 (m, 4H, Ar<sub>Ph</sub>H), 7.07 (dd, *J* = 11.8, 5.4 Hz, 4H, Ar<sub>Ph</sub>H), 4.24 (q, *J* = 7.1 Hz, 4H, NCH<sub>2</sub>CH<sub>3</sub>), 1.27 (t, *J* = 7.1 Hz, 6H, NCH<sub>2</sub>CH<sub>3</sub>). <sup>13</sup>C NMR (126 MHz, CDCl<sub>3</sub>) δ

154.39 (Se=C), 164.02, 162.03, 132.46, 132.39, 124.05, 124.02, 116.14, 115.97 (Ar<sub>Ph</sub>C), 129.03 (NC=CN), 42.65 (NCH<sub>2</sub>CH<sub>3</sub>), 14.38 (NCH<sub>2</sub>CH<sub>3</sub>). ESI-MS (+) [m/z]: 415.5 [M+Na]<sup>+</sup>, 313.8 [M-Se]<sup>+</sup>. Purity: 98.0% (by HPLC). Retention time t<sub>R</sub> = 10.628 min.

*1-ethyl-4,5-bis(4-fluorophenyl)-3-(2,4,6-trimethylbenzyl)-imidazole-2-selenone 2g*: white powder (yield 40.4%). <sup>1</sup>H NMR (500 MHz, CDCl<sub>3</sub>) δ 7.17 - 7.08 (m, 2H, Ar<sub>Ph</sub>H), 7.04 - 6.96 (m, 2H, Ar<sub>Ph</sub>H), 6.64 (dd, *J* = 6.9, 3.9 Hz, 4H, Ar<sub>Ph</sub>H), 6.58 (s, 2H, Ar<sub>Ph</sub>H), 5.60 (s, 2H, NCH<sub>2</sub>Ar), 4.27 (q, *J* = 7.1 Hz, 2H, NCH<sub>2</sub>CH<sub>3</sub>), 2.17 (s, 3H, ArCH<sub>3</sub>), 1.93 (s, 6H, ArCH<sub>3</sub>), 1.27 (t, *J* = 5.5 Hz, 3H, NCH<sub>2</sub>CH<sub>3</sub>). <sup>13</sup>C NMR (126 MHz, CDCl<sub>3</sub>) δ 156.70 (Se=C), 163.95, 163.63, 161.96, 161.64, 137.13, 136.86, 129.94, 129.73, 129.61, 129.08, 123.90, 123.87, 123.85, 123.82, 115.95, 115.78, 114.73, 114.56 (Ar<sub>Ph</sub>C), 132.40, 132.34, 132.14, 132.07 (NC=CN), 48.27 (NCH<sub>2</sub>Ar), 42.96 (NCH<sub>2</sub>CH<sub>3</sub>), 29.68, 20.65, 20.27 (ArCH<sub>3</sub>), 14.39 (NCH<sub>2</sub>CH<sub>3</sub>). ESI-MS (+) [m/z]: 417.0 [M-Se]<sup>+</sup>. Purity: 95.2% (by HPLC). Retention time t<sub>R</sub> = 18.680 min.

*1-benzyl-3-ethyl-4,5-bis(4-fluorophenyl)-imidazole-2-selenone 2h*: white powder (yield 99.8%). <sup>1</sup>H NMR (500 MHz, CDCl<sub>3</sub>) δ 7.26-7.16 (m, 5H, Ar<sub>Ph</sub>H), 7.05 (t, *J* = 8.6 Hz, 4H, Ar<sub>Ph</sub>H), 6.90 (d, *J* = 6.7 Hz, 4H, Ar<sub>Ph</sub>H), 5.48 (s, 2H, NCH<sub>2</sub>Ar), 4.30 (d, *J* = 7.1 Hz, 2H, NCH<sub>2</sub>CH<sub>3</sub>), 1.31 (t, *J* = 7.1 Hz, 3H, NCH<sub>2</sub>CH<sub>3</sub>). <sup>13</sup>C NMR (126 MHz, CDCl<sub>3</sub>) δ 156.84 (Se=C), 164.04, 163.98, 162.05, 161.99, 136.27, 129.51, 129.22, 128.40, 127.57, 127.47, 123.91, 123.88, 123.84, 123.81, 116.12, 115.95, 115.76, 115.59 (Ar<sub>Ph</sub>C), 132.67, 132.60, 132.45, 132.38 (NC=CN), 50.87 (NCH<sub>2</sub>Ar), 43.11 (NCH<sub>2</sub>CH<sub>3</sub>), 14.37 (NCH<sub>2</sub>CH<sub>3</sub>). ESI-MS (+) [m/z]: 454.9 [M+H]<sup>+</sup>, 476.9 [M+Na]<sup>+</sup>. Purity: 95.8% (by HPLC). Retention time t<sub>R</sub> = 10.923 min.

*1-ethyl-4,5-bis(4-fluorophenyl)-3-(2-methoxyethyl)-imidazole-2-selenone 2i*: white powder (yield 40.4%). <sup>1</sup>H NMR (500 MHz, CDCl<sub>3</sub>) δ 7.21 (ddd, *J* = 19.3, 8.3, 5.4 Hz, 4H, Ar<sub>Ph</sub>H), 7.09 - 6.99 (m, 4H, Ar<sub>Ph</sub>H), 4.31 (t, *J* = 5.6 Hz, 2H, NCH<sub>2</sub>CH<sub>2</sub>), 4.24 (q, *J* = 7.1 Hz, 2H, NCH<sub>2</sub>CH<sub>3</sub>), 3.81 (t, *J* = 5.6 Hz, 2H, NCH<sub>2</sub>CH<sub>2</sub>), 3.22 (s, 3H, OCH<sub>3</sub>), 1.27 (t, *J* = 7.1 Hz, 3H, NCH<sub>2</sub>CH<sub>3</sub>). <sup>13</sup>C NMR (126 MHz, CDCl<sub>3</sub>) δ 154.89 (Se=C), 164.01, 163.99, 162.02, 162.00, 133.10, 133.03, 132.53, 132.46, 124.12,

124.10, 123.95, 123.92, 116.09, 115.92, 115.81, 115.64 ( $\text{Ar}_{\text{Ph}}\text{C}$ ), 130.18, 128.74 ( $\text{NC}=\text{CN}$ ), 69.65 ( $\text{CH}_2\text{OCH}_3$ ), 58.61 ( $\text{CH}_2\text{OCH}_3$ ), 46.77 ( $\text{NCH}_2\text{CH}_2$ ), 42.69 ( $\text{NCH}_2\text{CH}_3$ ), 14.31 ( $\text{NCH}_2\text{CH}_3$ ). ESI-MS (+) [m/z]: 422.9 [M+H]<sup>+</sup>, 343.0 [M-Se]<sup>+</sup>. Purity: 99.3% (by HPLC). Retention time  $t_{\text{R}}$  = 15.602 min.

*1-ethyl-4,5-bis(4-fluorophenyl)-3-(3-hydroxypropyl)-imidazole-2-selenone 2j*: white powder (yield 56%). <sup>1</sup>H NMR (500 MHz, CDCl<sub>3</sub>)  $\delta$  7.24 - 7.15 (m, 4H,  $\text{Ar}_{\text{Ph}}\text{H}$ ), 7.07 (td,  $J$  = 8.5, 1.4 Hz, 4H,  $\text{Ar}_{\text{Ph}}\text{H}$ ), 4.46 - 4.41 (m, 2H,  $\text{NCH}_2\text{CH}_2\text{CH}_2\text{OH}$ ), 4.24 (q,  $J$  = 7.1 Hz, 2H,  $\text{NCH}_2\text{CH}_3$ ), 3.75 (t,  $J$  = 7.2 Hz, 1H, -OH), 3.51 (dd,  $J$  = 11.3, 6.5 Hz, 2H,  $\text{NCH}_2\text{CH}_2\text{CH}_2\text{OH}$ ), 1.61 (dt,  $J$  = 11.4, 5.8 Hz, 2H,  $\text{NCH}_2\text{CH}_2\text{CH}_2\text{OH}$ ), 1.26 (t,  $J$  = 7.1 Hz, 3H,  $\text{NCH}_2\text{CH}_3$ ). <sup>13</sup>C NMR (126 MHz, CDCl<sub>3</sub>)  $\delta$  154.84 ( $\text{Se}=\text{C}$ ), 164.09, 162.10, 132.50, 132.47, 132.43, 132.40, 123.70, 123.67, 123.65, 123.62, 116.28, 116.23, 116.10, 116.05 ( $\text{Ar}_{\text{Ph}}\text{C}$ ), 129.70, 129.17 ( $\text{NC}=\text{CN}$ ), 57.19 ( $\text{NCH}_2\text{CH}_2\text{CH}_2\text{OH}$ ), 43.60 ( $\text{NCH}_2\text{CH}_2\text{CH}_2\text{OH}$ ), 42.96 ( $\text{NCH}_2\text{CH}_3$ ), 32.29 ( $\text{NCH}_2\text{CH}_2\text{CH}_2\text{OH}$ ), 14.36 ( $\text{NCH}_2\text{CH}_3$ ). ESI-MS (+) [m/z]: 423.0 [M+H]<sup>+</sup>, 343.2 [M-Se]<sup>+</sup>. Purity: 98.7% (by HPLC). Retention time  $t_{\text{R}}$  = 14.745 min.

*4,5-di([1,1'-biphenyl]-4-yl)-1,3-diethyl-imidazole-2-selenone 2k*: white powder (yield 77.3%). <sup>1</sup>H NMR (500 MHz, CDCl<sub>3</sub>)  $\delta$  7.60 (d,  $J$  = 8.0 Hz, 8H,  $\text{Ar}_{\text{Ph}}\text{H}$ ), 7.45 (t,  $J$  = 7.5 Hz, 4H,  $\text{Ar}_{\text{Ph}}\text{H}$ ), 7.38 (t,  $J$  = 7.4 Hz, 2H,  $\text{Ar}_{\text{Ph}}\text{H}$ ), 7.32 (d,  $J$  = 8.1 Hz, 4H,  $\text{Ar}_{\text{Ph}}\text{H}$ ), 4.33 (q,  $J$  = 7.0 Hz, 4H,  $\text{NCH}_2\text{CH}_3$ ), 1.34 (t,  $J$  = 7.1 Hz, 6H,  $\text{NCH}_2\text{CH}_3$ ). <sup>13</sup>C NMR (126 MHz, CDCl<sub>3</sub>)  $\delta$  154.08 ( $\text{Se}=\text{C}$ ), 141.71, 139.86, 130.93, 128.89, 127.83, 127.33, 127.06, 126.99 ( $\text{Ar}_{\text{Ph}}\text{C}$ ), 129.69 ( $\text{NC}=\text{CN}$ ), 42.75 ( $\text{NCH}_2\text{CH}_3$ ), 14.53 ( $\text{NCH}_2\text{CH}_3$ ). ESI-MS (+) [m/z]: 429.0 [M-Se]<sup>+</sup>. Purity: 99.0% (by HPLC). Retention time  $t_{\text{R}}$  = 19.544 min.

*1,3-diethyl-4,5-bis(4'-fluoro-[1,1'-biphenyl]-4-yl)-imidazole-2-selenone 2l*: white powder (yield 46.0%). <sup>1</sup>H NMR (500 MHz, CDCl<sub>3</sub>)  $\delta$  7.55 (dd,  $J$  = 9.1, 5.1 Hz, 8H,  $\text{Ar}_{\text{Ph}}\text{H}$ ), 7.34 - 7.29 (m, 4H,  $\text{Ar}_{\text{Ph}}\text{H}$ ), 7.14 (t,  $J$  = 8.6 Hz, 4H,  $\text{Ar}_{\text{Ph}}\text{H}$ ), 4.32 (q,  $J$  = 7.0 Hz, 4H,  $\text{NCH}_2\text{CH}_3$ ), 1.33 (t,  $J$  = 7.0 Hz, 6H,  $\text{NCH}_2\text{CH}_3$ ). <sup>13</sup>C NMR (126 MHz, CDCl<sub>3</sub>)  $\delta$  154.23 ( $\text{Se}=\text{C}$ ), 163.72, 161.75, 140.74, 135.99, 135.97, 130.99, 128.65, 128.58, 127.20, 127.07, 115.92, 115.75 ( $\text{Ar}_{\text{Ph}}\text{C}$ ), 129.60 ( $\text{NC}=\text{CN}$ ), 42.75 ( $\text{NCH}_2\text{CH}_3$ ), 14.53 ( $\text{NCH}_2\text{CH}_3$ ). ESI-MS (+) [m/z]: 465.2 [M-Se]<sup>+</sup>. Purity: 97.2% (by HPLC).

---

Retention time  $t_R$  = 11.632 min.

*1,3-diethyl-4,5-bis(4'-methoxy-[1,1'-biphenyl]-4-yl)-imidazole-2-selenone 2m*: white powder (yield 84.4%).  $^1\text{H}$  NMR (500 MHz,  $\text{DMSO-}d_6$ )  $\delta$  7.66 (dd,  $J$  = 11.7, 8.5 Hz, 8H,  $\text{Ar}_{\text{Ph}}\text{H}$ ), 7.46 (d,  $J$  = 8.2 Hz, 4H,  $\text{Ar}_{\text{Ph}}\text{H}$ ), 7.01 (d,  $J$  = 8.7 Hz, 4H,  $\text{Ar}_{\text{Ph}}\text{H}$ ), 4.13 (q,  $J$  = 6.9 Hz, 4H,  $\text{NCH}_2\text{CH}_3$ ), 3.79 (s, 6H,  $\text{OCH}_3$ ), 1.16 (t,  $J$  = 7.0 Hz, 6H,  $\text{NCH}_2\text{CH}_3$ ).  $^{13}\text{C}$  NMR (126 MHz,  $\text{CDCl}_3$ )  $\delta$  153.82 ( $\text{Se}=\text{C}$ ), 159.54, 141.25, 132.33, 130.91, 128.05, 126.79, 126.40, 114.33 ( $\text{Ar}_{\text{Ph}}\text{C}$ ), 129.73 ( $\text{NC}=\text{CN}$ ), 55.36 ( $\text{ArOCH}_3$ ), 42.72 ( $\text{NCH}_2\text{CH}_3$ ), 14.55 ( $\text{NCH}_2\text{CH}_3$ ). ESI-MS (+) [ $m/z$ ]: 489.2 [ $\text{M-Se}$ ] $^+$ . Purity: 97.2% (by HPLC). Retention time  $t_R$  = 11.949 min.

### 2.2.3. Synthesis of **2n**

*1,3-diethyl-imidazole-2-selenone 2n*: **1n** (686 mg, 3.31 mmol) was dissolved in water (20 mL). Selenium powder (400 mg, 5.06 mmol) along with  $\text{Na}_2\text{CO}_3$  (920 mg, 6.66 mmol) were then added and the reaction mixture was heated to reflux for 5 h. The reaction mixture was filtered through celite, washed with distilled water and was extracted using ethyl acetate. A white powder (403 mg, yield 60%) was obtained under vacuum.  $^1\text{H}$  NMR (500 MHz,  $\text{CDCl}_3$ )  $\delta$  6.89 (d,  $J$  = 2.0 Hz, 2H,  $\text{CH}=\text{CH}$ ), 4.18 (qd,  $J$  = 7.2, 1.9 Hz, 4H,  $\text{NCH}_2\text{CH}_3$ ), 1.39 (td,  $J$  = 7.3, 2.0 Hz, 6H,  $\text{NCH}_2\text{CH}_3$ ).  $^{13}\text{C}$  NMR (126 MHz,  $\text{CDCl}_3$ )  $\delta$  154.06 ( $\text{Se}=\text{C}$ ), 118.07 ( $\text{NC}=\text{CN}$ ), 44.64 ( $\text{NCH}_2\text{CH}_3$ ), 14.46 ( $\text{NCH}_2\text{CH}_3$ ). ESI-MS (+) [ $m/z$ ]: 204.0 [ $\text{M}+\text{H}$ ] $^+$ , 125.5 [ $\text{M-Se}$ ] $^+$ . Purity: 98.7% (by HPLC). Retention time  $t_R$  = 11.452 min.

### 2.3. Cell culture

Human hepatocellular carcinoma cell line HepG2 was obtained from the American Type Culture Collection (ATCC) and maintained in DMEM (Gibco, USA) supplemented with 10% FBS and 1% penicillin/streptomycin. Human ovarian cancer cell line A2780 and Human immortalized ovarian epithelial cell line IOSE80 were purchased from iCell Bioscience Inc (Shanghai, China) and were grown in RPMI 1640 medium (Gibco, USA) supplemented with 10% FBS and 1% penicillin/streptomycin. All cells reached a maximum of 20 passages during these studies.

---

#### 2.4. Cell viability assay

**2a-2n** and ebselen were dissolved in DMF to prepare a 20 mM stock solution. Then, the solutions were diluted with cell culture medium before treatment. Cells in the logarithmic growth phase were cultured into 96-well plates overnight and then incubated with the **2a-2n** and ebselen at 37 °C and 5% CO<sub>2</sub> for 72 hours. The cell viability was detected by the MTT assay. MTT (5 mg/mL in PBS solution) were added to each well. After incubating for four hours, the medium was removed and 200 μL DMSO were added to dissolve formazan. Finally, the absorbance data of each well was detected at 490 nm after shaking on the shaker for 10 minutes.

#### 2.5. Isolated TrxR enzyme assay

Different concentrations of **2b** (5 μM, 10 μM, 20 μM, 40 μM) and TrxR were successively dissolved in reaction buffer, DMF was used as a control. 200 μL of the reaction buffer and 25 μL of NADPH solution were then added to each well. Subsequently, 25 μL of DTNB (20 mM) solution was dropwise added to each well to start the reaction. After mixing, the absorbance data were recorded at 405 nm every 10 s for the first six minutes by microplate reader. The calculation method was according to our previously published methods (Fan et al., 2019).

#### 2.6. Apoptosis assays

A2780 cells were incubated with 0.1% DMF or **2b** in different concentrations for 48 h. Then A2780 cells were stained with Annexin V-FITC/PI reagent before detecting the double fluorescent signal by flow cytometry (BD Accuri™ C6).

#### 2.7. Cell cycle arrest

A2780 cells (6 x 10<sup>5</sup> cells/well) were cultured in 6-well plates for 24 h. Then, the cells were treated with **2b** for another 24 h. DMF group was as a control. Cells were harvested and processed using the DNA content kit (Nanjing Key Gen Biotech) according to the manufacturer's

---

protocol. Stage of the cell cycle was determined by flow cytometry (Beckman Gallios).

### 2.8. Intracellular ROS measurement

The fluorescent probe DCFH-DA (Beyotime, China) were used to assess the intracellular ROS generation. A2780 cells ( $1 \times 10^5$ ) were evenly seeded in 6-well plate and cultured overnight. After adhering to the wall, cells were treated with DMF or indicated concentrations of **2b** and cultured for another 6 h. Then, cells were rinsed gently with PBS and DCFH-DA ROS probe (Beyotime, China) was loaded by the kit method. At last, cells were washed twice with PBS before visualizing intracellular fluorescence generation by a fluorescent microscopy (Leica DMI8) under 200 $\times$ magnification.

For quantitative measurement of ROS production in A2780 and IOSE80 cells, cells were plated in 96-well plate at a density of 8000 cells per well, incubated for 24 h before treatment with the indicated concentrations of **2b** for 6 h. Then, cells were treated with fluorescent probe DCFH2-DA by the same method mentioned above and the fluorescence intensity was tested by a microplate reader (Tecan M1000 Pro).

### 2.9. Assessment of MMP

MMP (mitochondrial membrane potential) was detected by the JC-1 dye. A2780 cells were cultured in a 6-well plate and washed by PBS. Then cells were stained with 5  $\mu$ M JC-1 for 15min in darkness. Then remained dye was washed by PBS and red/green fluorescence were observed by a fluorescent microscopy (Leica DMI8).

### 2.10. Intracellular GSH/GSSG ratio Measurement

After incubating with **2b** for 24 h in A2780 cells, GSH and GSSG Assay Kit (Beyotime, China) was used to measure the ratio of GSH/GSSG.

### 2.11. UV-Vis spectral analysis

**2b** was dissolved in DMF in a concentration of 20 mM and ct-DNA was dissolved in PBS buffer

---

with pH 7.2 in a concentration of 1.152 mM. **2b** was diluted 4000 times to obtain a solution in a concentration of 20  $\mu$ M. Next, the ct-DNA solution was gradually dropped into **2b** solution mentioned above. The data of absorption spectra were recorded by spectrophotometer.

#### 2.12. Circular dichroism spectral analysis

**2b** was incubated with ct-DNA ( $1.0 \times 10^{-5}$  M) at 37 °C overnight. The data of **2b** with different concentrations (0, 0.05, 0.1, 0.2, 0.5, 0.8, 1.0,  $2.0 \times 10^{-5}$  M) was recorded range from 235 nm to 300 nm by CD spectrometer.

#### 2.13. Stability analysis

**2b** was dissolved in 10% deuterioxide + 90% dimethyl sulfoxide- $d_6$  and then detected  $^1\text{H}$  NMR spectra in 7 days.

#### 2.14. Interaction with GSH and NAC

**2b** (2 mM) and GSH (2 mM) were dissolved in dimethyl sulfoxide- $d_6$  and then detected  $^1\text{H}$  NMR spectra in 7 days.

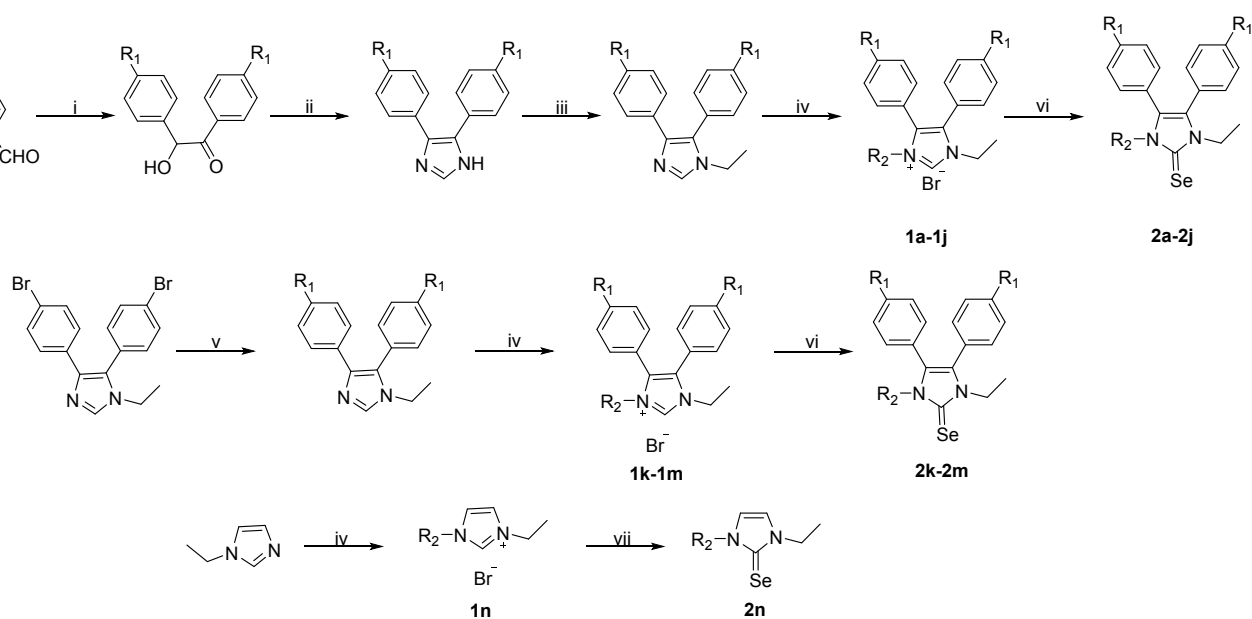
**2b** (2 mM) and NAC (2 mM) were dissolved in 50% acetonitrile- $d_3$  + 50% dimethyl sulfoxide- $d_6$  and then detected  $^1\text{H}$  NMR spectra in 7 days.

#### 2.15. X-ray crystallographic analysis

The data of **2b** and **2l** were collected at 193(2) K and 292(2) K on a BRUKER Smart APEX II CCD area-detector diffractometer, respectively. CCDC 2051718 and 2052871. DOI: 10.5517/ccdc.csd.cc26vzgj and 10.5517/ccdc.csd.cc26x5nz.

### 3. Results and discussion

#### 3.1. Chemistry



compounds	R <sub>1</sub>	R <sub>2</sub>	compounds	R <sub>1</sub>	R <sub>2</sub>
1a, 2a	OMe	Et	1h, 2h	F	
1b, 2b	OMe		1i, 2i	F	MeO
1c, 2c	OMe		1j, 2j	F	HO
1d, 2d	OMe	MeO	1k, 2k		Et
1e, 2e	Br	Et	1l, 2l		Et
1f, 2f	F	Et	1m, 2m		Et
1g, 2g	F		1n, 2n	-	Et

**Scheme 1.** i: thiamine hydrochloride, rt, ii: formamide, 210 °C, reflux, iii: NaH, ethyl bromide, THF, reflux, iv: R<sub>2</sub>Br, CH<sub>3</sub>CN, reflux, 85 °C, 2 d, v: K<sub>2</sub>CO<sub>3</sub>, Pd(PPh<sub>3</sub>)<sub>4</sub>, ethanol/ H<sub>2</sub>O/acetone (3:2:3), reflux, 95 °C, 2 d, vi: Se, KOtBu, THF, 0 °C, 5 h, vii: Se, Na<sub>2</sub>CO<sub>3</sub>, H<sub>2</sub>O, 100 °C, reflux, 5 h.

The 4,5-diarylimidazole salts **1a-1n** in the **Scheme 1** were synthesized according to our previously published methods (Fan et al., 2019). In general, benzoin condensation reactions were carried out to obtain diketone derivatives by anisaldehyde analogues, and then the products were cyclized with formamide to obtain imidazole derivatives. Two-step substitution reactions of the imidazole rings were then carried out to obtain 4,5-diarylimidazole salts. In addition, biphenyl imidazole compounds were first obtained by

suzuki coupling reaction. Subsequently, the imidazole salt ligands (**1a-1n**) were dissolved in tetrahydrofuran (THF) and reacted with elemental Se powder under the alkaline condition of potassium tert-butoxide (KOtBu) to obtain the corresponding Se-NHC compounds **2a-2n** (Weiss, Reichel, Handke, & Hampel, 1998). The obtained compounds were characterized by  $^1\text{H}$  NMR,  $^{13}\text{C}$  NMR, and mass spectra (**Figure S4** and **S6**). The chemical shift value of the carbene H-atoms for **2a-n** disappeared compared to 4,5-diarylimidazole salts **1a-n** in the  $^1\text{H}$  NMR spectra. In  $^{13}\text{C}$  NMR spectra, the chemical shift value of C=Se for **2a-n** was in the range of 150-160 ppm which was increased by approximately 15-25 ppm compared to the 4,5-diarylimidazole salts **1a-n**. In addition, positive mode ESI mass spectrometry showed that Se-NHC compounds documented a peak corresponding to the  $[\text{M-Se}]^+$  fragment for **2a-2n**.

### 3.2. Crystal Structure Description

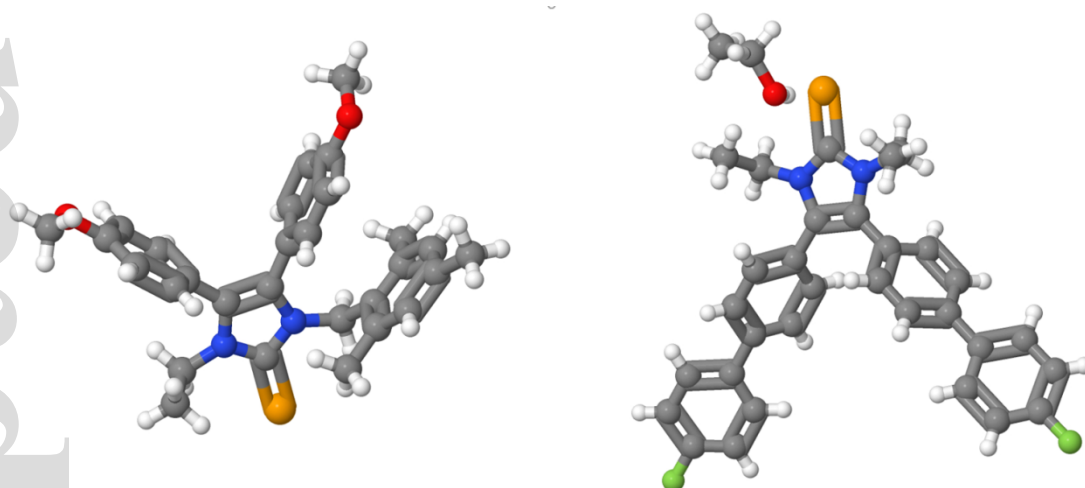


**Fig 2.** The crystal structure of **2b** (left) and **2l** (right).

To gain insight into the structural information of these compounds, **2b** and **2l** were isolated as single crystals and characterized by X-ray diffraction. The molecular structures of **2b** and **2l** were depicted in **Figure 2** and **Table S1-S10**. The compound **2b** was crystallized in dichloromethane and *n*-hexane in a monoclinic  $P2_1/c$  space group:  $a =$

11.4140 (5) Å; b = 12.8499 (6) Å; c = 17.9400 (8) Å;  $\alpha = 90^\circ$ ;  $\beta = 95.821 (2)^\circ$ ;  $\gamma = 90^\circ$ ; V = 2617.7 (2) Å<sup>3</sup>; Z = 4 (**Table S1**). The selected bond lengths and bond angles were given in **Table S3**. Meanwhile, the bond angle was different between N(1) and N(2) side chain: C(12)-C(11)-N(1), 110.0(3) and N(2)-C(13)-C(14), 114.00(19).

The compound **2I** was crystallized in dichloromethane and ethanol in a monoclinic P2<sub>1</sub>/c space group: a = 16.710 (3) Å; b = 10.2283 (16) Å; c = 17.708 (3) Å;  $\alpha = 90^\circ$ ;  $\beta = 106.116 (3)^\circ$ ;  $\gamma = 90^\circ$ ; V = 2907.6(8) Å<sup>3</sup>; Z = 4 (**Table S6**). The bond angle of C(151)-N(11)-C (221) and C(151)-N(21)-C(241) in **2I** were both 124.0(3) which was different from **2b** (**Table S8**). The bond lengths of C=Se [1.843(3) and 1.842(4)] are higher than that of general C-N, C-C, and C-O, and are equivalent to the C=Se bond length in known compounds (1.868(3)), which are 1.84(3) (Nelson et al., 2014; Seliman et al., 2017).

### 3.3. Reaction with GSH and NAC

The stability of Se-NHC compounds under physiological conditions is crucial for biological studies. Hence, the reactivity of the Se-NHC compound **2b** in the presence of physiologically important thiols like GSH and NAC, were measured by <sup>1</sup>H NMR spectra (**Figure S1** and **S2**). The results showed that none of the new peaks appeared in the <sup>1</sup>H NMR spectra with GSH and NAC during 7 days, indicating that **2b** was relatively stable under the environment of physiologically important thiols. The <sup>1</sup>H NMR spectra of **2b** in deuterioxide was tested as a control and no significant changes were observed, indicating that **2b** was relatively stable in deuterioxide (**Figure S3**). Above all, we confirmed that **2b** could stay stable under physiological conditions.

3.4 *In vitro* cytotoxic activities of selenium compounds (2a-2n)

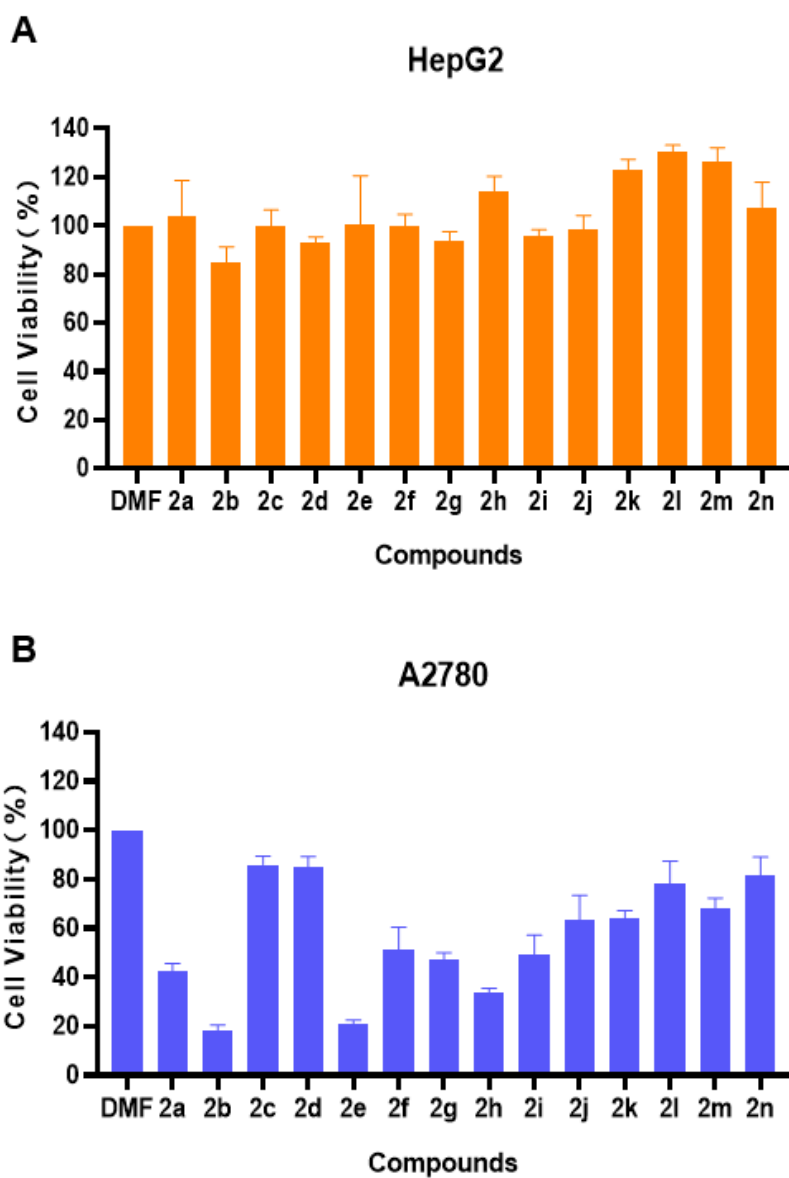


**Fig 3.** Antiproliferative activity of Se-NHC compounds in HepG2 (A) and A2780 (B) cells at a dose of 20  $\mu$ M. The results are mean  $\pm$  SD of three independent experiments.

---

MTT assay is known as a general experiment to validate the cytotoxicity effect of tested compounds and it is also a classical method for screening potential anticancer agents. Thus, *in vitro* cytotoxicity assays were performed by MTT assay to get an insight into the antitumor activity of the Se-NHC compounds. Initially, we tested the antitumor activity of Se-NHC compounds **2a-2n** at the same concentration (20  $\mu$ M) in HepG2 HCC cells and A2780 ovarian cancer cells by MTT assays. As shown in **Figure 3A** and **3B**, all Se-NHC compounds have no inhibitory effects in HepG2 cell line while several compounds including **2b**, **2e**, and **2h** show good antiproliferative effects against A2780 cells. These results indicated that there was a hint of selectivity of these Se-NHC compounds towards A2780 cells.

Subsequently, we determined the IC<sub>50</sub> values of **2a-2n** in A2780 human ovarian cancer cells and IOSE80 human normal ovarian epithelial cells. Ebselen was used as a positive control. As can be seen from **Table 1**, several compounds (**2a**, **2b**, **2g**, **2e**, **2h**) exhibited effective antitumor activity. Among them, antitumor activities of **2a**, **2b** and **2h** were up to 2.6-fold (**2a**, 9.7  $\mu$ M), 4-fold (**2b**, 6.4  $\mu$ M) and 2-fold (**2h**, 13.0  $\mu$ M) more active than ebselen (25.4  $\mu$ M). Notably, ebselen and most active compounds which exhibited effective activities against A2780 cells showed weak cytotoxicity in IOSE80 normal cells. Above all, these compounds performed equivalent or better selectivity towards cancer cells A2780 than ebselen.

Hence, we have summarized an SAR study for this series of compounds. As shown in **Table 1**, biphenyl Se-NHC compounds **2k**, **2l** and **2m** as well as imidazole Se-NHC compound **2n** showed little cytotoxicity against A2780 cells compared with most 4,5-diphenylimidazole Se-NHC compounds. These results suggested that the benzene ring at the 4 and 5 positions of the imidazole ring was necessary for bioactivity and larger steric hindrance substituents like biphenyls could reduce the antiproliferative activity. Next, Se-NHC compounds **2a** (9.7  $\pm$  1.41  $\mu$ M), **2e** (21.1  $\pm$  2.02  $\mu$ M), and **2k** (>160  $\mu$ M) showed decreasing antiproliferative activities against A2780 cells indicating that the inhibitory activity was related to the substituents at the *para* position of the benzene ring (inhibitory

activity: Ph < Br < OMe). In addition, compounds with an N(2) -aromatic chain [**2b** ( $6.4 \pm 1.21 \mu\text{M}$ ), **2g** ( $19.1 \pm 3.23 \mu\text{M}$ ), **2h** ( $13.0 \pm 1.79 \mu\text{M}$ ) except for **2c** ( $>160 \mu\text{M}$ )] showed the same or more active inhibitory effects than those with -aliphatic chains. These results indicated that the aromatic ring on the *N* side chain played a significant role in anticancer activities and it may be attributed to the lipophilicity of the compounds.

Table 1. Antiproliferative effects of **2a-2n** against A2780 and IOSE80 Cells after 72 h of Incubation.

Compounds	IC <sub>50</sub> (μM) Mean ± SD		SI <sup>a</sup>
	A2780	IOSE80	
Ebselen	25.4 ± 2.80	55.4 ± 8.45	2.18
<b>2a</b>	9.7 ± 1.41	51.3 ± 4.86	5.30
<b>2b</b>	6.4 ± 1.21	11.0 ± 2.40	1.72
<b>2c</b>	> 160	> 160	-
<b>2d</b>	> 160	> 160	-
<b>2e</b>	21.1 ± 2.02	43.7 ± 3.87	2.05
<b>2f</b>	85.3 ± 8.63	> 160	-
<b>2g</b>	19.1 ± 3.23	34.8 ± 3.06	1.83
<b>2h</b>	13.0 ± 1.79	29.4 ± 2.86	2.26
<b>2i</b>	34.6 ± 1.50	43.4 ± 7.40	1.26
<b>2j</b>	> 160	> 160	-
<b>2k</b>	> 160	> 160	-
<b>2l</b>	> 160	> 160	-
<b>2m</b>	> 160	> 160	-
<b>2n</b>	> 160	> 160	-

<sup>a</sup> SI, Selectivity index,  $SI = IC_{50}(\text{IOSE80}) / IC_{50}(\text{A2780})$ .

These results indicated that Se-NHC compounds showed selectivity towards A2780 ovarian cancer cells and these compounds were not sensitive in HepG2 cells. Among them, compound **2b** exhibited the best antitumor activity against A2780 cells. Moreover, all of Se-NHC compounds

---

demonstrated selectivity towards A2780 human ovarian cancer cells than IOSE80 human normal ovarian epithelial cells. The SAR studies also provide some ideas for our later design, such as expanding the aromaticity of the substituents on the *N* side chain of the imidazole ring or introducing aliphatic substituents at the *para* positions of the 4,5-diaryl groups which may improve the antiproliferative activity of Se-NHC compounds.

### 3.5. The isolated TrxR inhibition and interaction with ct-DNA

Se compounds have been well documented to show higher selectivity and sensitivity in cancer cells and exhibited pro-oxidant properties which can be broadly attributed to different targets such as protein thiols and DNA binding (Gandin, Khalkar, Braude, & Fernandes, 2018). Selenoprotein such as TrxR has been considered to be a potential target for selenium compounds (He, Ji, Lai, & Chen, 2015; Y. W. Liang, Zheng, Li, Zheng, & Chen, 2014). Thus, we studied the TrxR inhibitory effect and DNA binding affinity of **2b**. Unexpectedly, **2b** showed weak TrxR inhibitory activity ( $IC_{50} > 40 \mu\text{M}$ ) on isolated enzymes using the DTNB assay in **Figure 4A**, indicating that TrxR is not the potential target of **2b**. Similarly, the absorption of DNA was not changed (**Figure 4B**) and the configuration of DNA did not change significantly by circular dichroism (CD) assay with an increase of **2b** concentration (**Figure 4C**), which also indicated that DNA is not the target of these Se-NHC compounds.

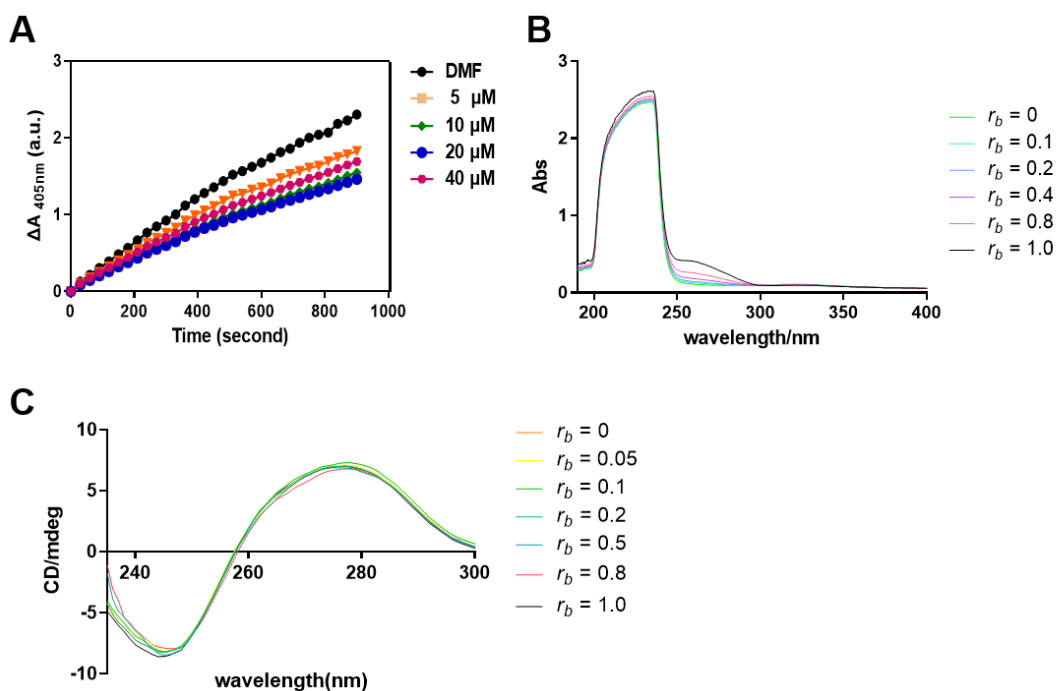


**Fig 4.** Inhibition to the activity of purified TrxR by **2b** (A); UV/Vis spectra (B) and CD spectra (C) recorded for the reaction of compound **2b** with ct-DNA.  $r_b = [\mathbf{2b}]/[\text{ct-DNA}]$ .

The above negative results revealed that Se-NHC compounds did not directly interact with selenoprotein or DNA to exert antitumor activity. Previous studies have shown that Se compounds were able to alter the intracellular redox balance and a slight additional ROS induction would lead to oxidative stress dependent cell death in tumor microenvironment (Cairns, Harris, & Mak, 2011; Gorrini, Harris, & Mak, 2013; Khalkar et al., 2018; Selenius et al., 2012). Hence, the mechanisms related to tumor cell apoptosis caused by elevated ROS have been another direction for us to study the mode of action of Se-NHC compounds.

### 3.6. ROS analysis

Maintaining redox homeostasis is necessary for all healthy cells. The balance between the generation of ROS and their elimination by cellular antioxidant agents plays an important role in cellular events. In addition, the level of ROS in tumor cells is excessively increased because of the aberrant proliferation of cancer cells (Gorrini et al., 2013; Sze et al., 2020). It was reported that the antitumor effect of organoselenium compounds is

---

related to the level of ROS (An, Zhang, et al., 2018; Deng, Yu, Cao, Zheng, & Chen, 2015; Dos Santos et al., 2020; Fernandes & Gandin, 2015; Gandin et al., 2018; He et al., 2015; Y. Liang, Zhou, Deng, & Chen, 2016; Misra, Boylan, Selvam, Spallholz, & Bjornstedt, 2015; Yang, Deng, Zeng, Hu, & Chen, 2016; Zhao et al., 2017).

To investigate whether the proliferation inhibitory activity of **2b** was associated with ROS production, the level of ROS in **2b**-treated A2780 cells was detected by general methods in literature (Saleh et al., 2015). As shown in **Figure 5A**, A2780 cells were incubated with **2b** (10  $\mu$ M, 20  $\mu$ M, and 40  $\mu$ M) for 12 h and the ROS production was analyzed by fluorescence analysis. The ROS level in cells treated with **2b** was higher than control group. These findings suggested that **2b** can activate ROS in a dose-dependent manner in A2780 cells as expected. To demonstrate whether ROS was related to the selectivity towards A2780 cells, A2780 human ovarian cancer cells and IOSE80 human normal ovarian epithelial cells were incubated with **2b** in different concentrations (2.5  $\mu$ M, 5  $\mu$ M, 10  $\mu$ M, 20  $\mu$ M and 40  $\mu$ M) for 6 h and the production of ROS was measured by ROS assay kit. As shown in **Figure 5B**, the production of ROS increased in a dose-dependent manner in A2780 cells while the production of ROS in IOSE80 was not changed significantly with the concentration increased, even under a high dose (40  $\mu$ M). This result suggested that the antitumor activity of **2b** may be due to its ability to disrupt redox homeostasis in cancer cells and induce ROS accumulation, thereby leading to oxidative stress dependent cell death of cancer cells. Meanwhile, in normal cell IOSE80, **2b** displayed little ability to induce the accumulation of ROS and this may be the reason for its selectivity towards A2780 cells than IOSE80.

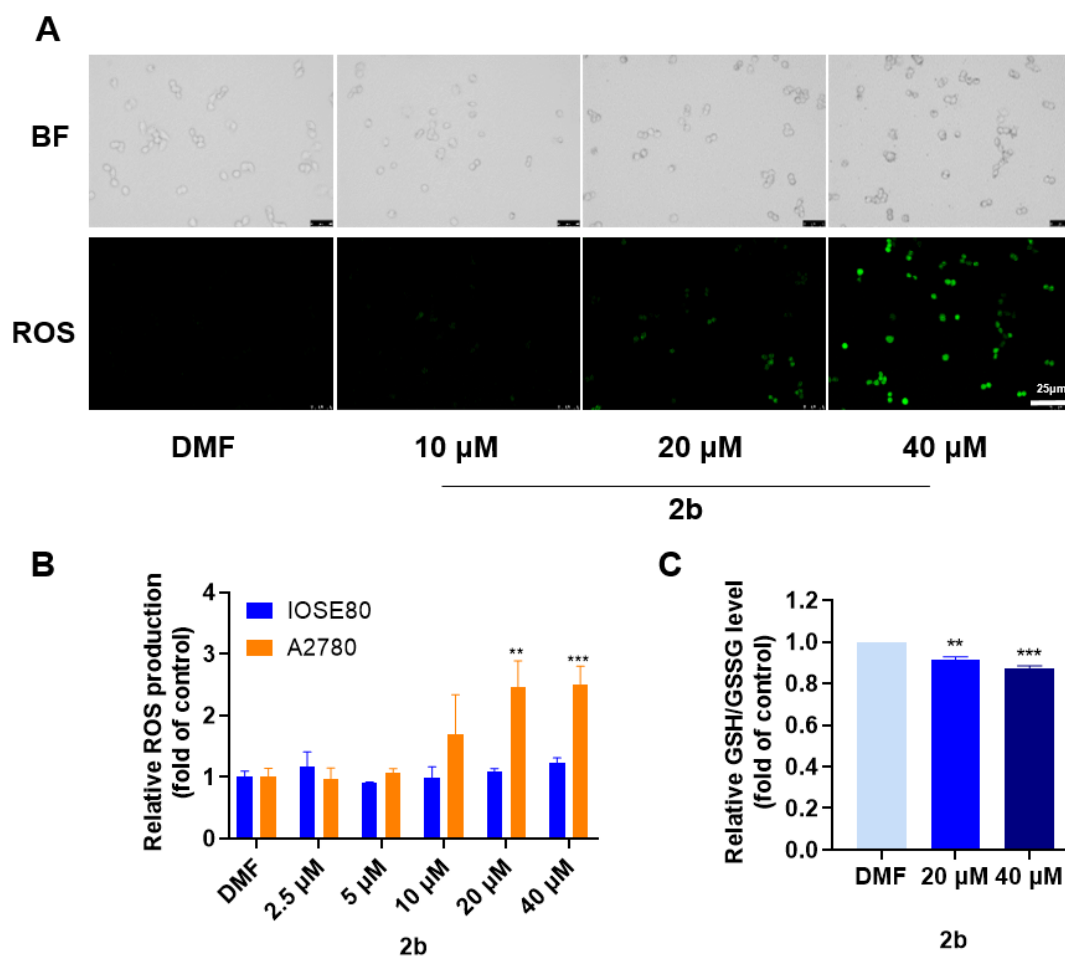


**Fig 5.** ROS generation after treatment with **2b** in different concentrations for 12 h (A, original magnification, 200 x); ROS production of IOSE80 and A2780 after treated with **2b** for 6 h (B). The ratio of GSH/GSSG in A2780 cells treated with **2b** for 24 h (C). \*\* $p < 0.01$  and \*\*\* $p < 0.001$  compared with group DMF.

It is well known that GSH/GSSG ratio was closely related to ROS level and it was usually selected as an indicator for antioxidant proteins and oxidative stress. (Lu et al., 2018). Therefore, we examined whether treatment with **2b** can affect the GSH/GSSG ratio. As shown in **Figure 5C**, **2b** can reduce the GSH/GSSG ratio in A2780 cells. The decreased GSH/GSSG ratio and increased production of ROS indicated that **2b** could disrupt the redox balance and lead to oxidative stress dependent cell death in A2780 cells.

### 3.7. MMP

It is well known that the major source of ROS comes from mitochondrial metabolism (Zhang, Li, Han, Liu, & Fang, 2017). The accumulation of ROS in cells can damage DNA through oxidative stress, destroy MMP and cause mitochondrial dysfunction, which ultimately leading to apoptosis and cell death (Bian, Fan, Zhao, & Liu, 2019; Dharmaraja, 2017; Huang et al., 2018; Pelicano, Carney, & Huang, 2004). MMP in A2780 cells treated with **2b** was tested by JC-1 kit. As shown in **Figure 6**, a dose-dependent decrease in MMP was observed (red fluorescence turning green fluorescence) indicating the normal physiological MMP was seriously damaged by **2b** in 40  $\mu\text{M}$ . This result suggested that **2b** can induce ROS production, damage MMP, and lead to mitochondrial dysfunction.

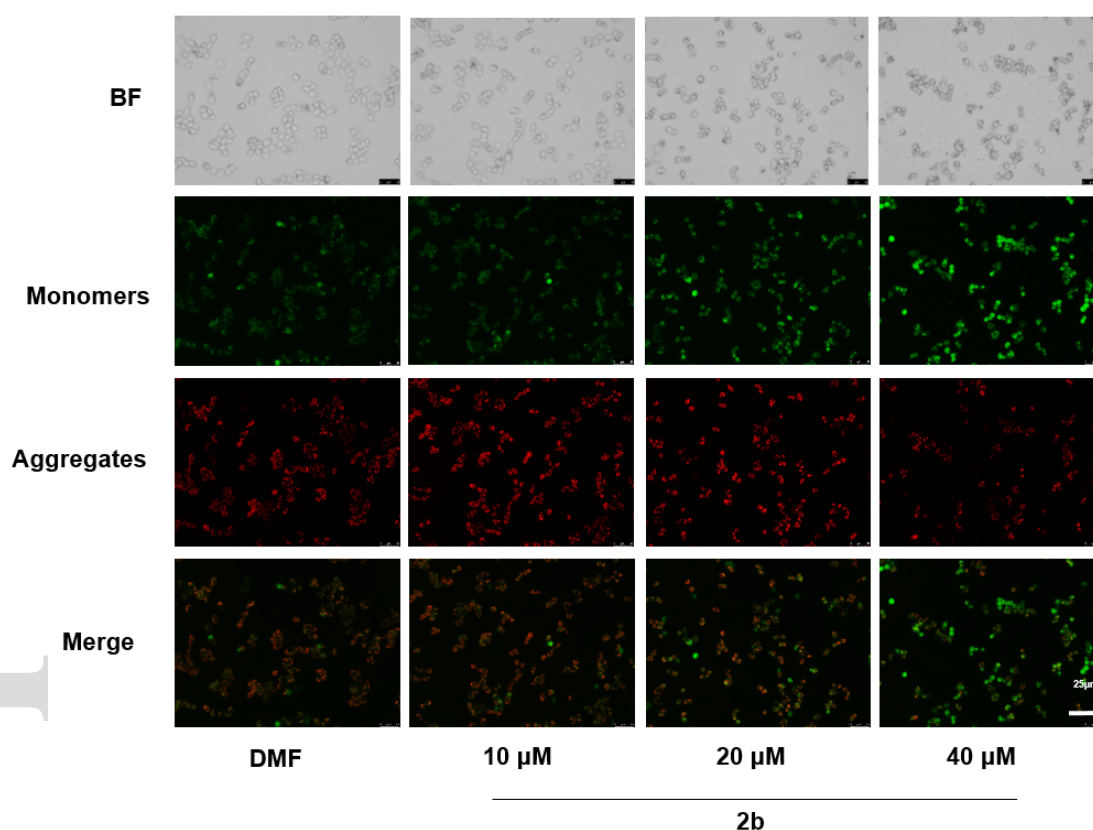


**Fig 6.** MMP imaged by JC-1 staining after treatment with **2b** for 24 h (original magnification, 200 x ).

### 3.8. Cell cycle analysis and apoptosis

The high level of ROS can cause oxidative stress on the cells, which may eventually lead to cell death or apoptosis (Bian et al., 2019). Therefore, we investigated whether the ROS production induced by **2b** in the A2780 cells could lead to apoptosis. Hence, the apoptosis of A2780 cells treated with **2b** was detected by propidium iodide (PI) staining and FITC-Annexin V staining (Fan et al., 2019). The A2780 cells were incubated with **2b** for 48 h and the state of apoptosis was measured by flow cytometry. As shown in **Figure 7A**, the apoptosis in **2b**-treated A2780 cells was enhanced in a dose-dependent manner. Subsequently, the cell cycle progression of **2b**-treated A2780 cells was studied by PI staining and the results showed that the cells were arrested at G0/G1 phase after treatment for 24 h. (**Figure 7B**). Thus, **2b** could block the A2780 cell cycle in the G0/G1 phase, and finally promote cell apoptosis.

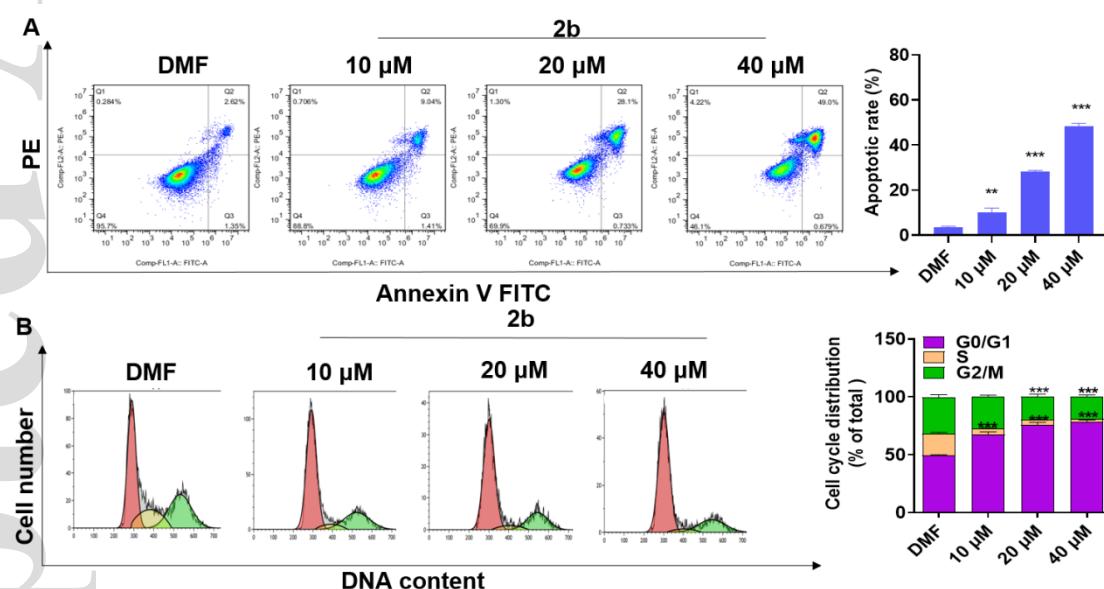


**Fig 7.** Apoptosis of A2780 cells treated with **2b** at different concentrations for 48 h (A); effect of **2b** on cell cycle progression (B). \*\* $p < 0.01$  and \*\*\* $p < 0.001$  compared with group DMF.

In our previous work, NHC complexes containing different transition metals derived from 4,5-diarylimidazole can inhibit the activity of TrxR and C-terminal thiol/selenol was the active site (Bian et al., 2020; Fan et al., 2019; Liu, Bendsdorf, Hagenbach, et al., 2011; Liu, Bendsdorf, & Proetto, 2011; Liu et al., 2012). We herein further introduced Se into NHC scaffold to synthesize fourteen Se-NHC compounds and evaluated their biological activity. Among them, compound **2b** with 2,4,6-trimethylbenzyl group on the N(2) side showed the

---

most potent cytotoxicity and provided a hint of selectivity towards A2780 cells. However, compound **2b** showed weak inhibition of the isolated TrxR which did not meet our original design and this stimulated us to search for the antitumor mechanism of Se-NHC compounds. Inspiringly, numbers of studies showed that Se compounds could induce ROS accumulation and promote cell apoptosis (Khalkar et al., 2018). Consequently, compound **2b** was selected for the following studies, and the action mechanism of compound **2b** in A2780 cells involved accumulation of ROS, mitochondrial dysfunction, and induction of apoptosis.

#### 4. Conclusion

A series of Se-NHC compounds were synthesized, characterized, and biologically investigated. A preliminary SAR study showed that compound **2b** exhibited an effective cytotoxic effect and selectivity towards A2780 cells. However, the TrxR and DNA were not the potential targets for Se-NHC compounds and the experiments showed that the cytotoxicity and selectivity were attributed to apoptosis activated by ROS. Studies demonstrated that **2b** mainly induced the accumulation of ROS, damaged the MMP, blocked the cells in the G0/G1 phase, and finally promoted A2780 cell apoptosis. All of the results indicated that **2b** represents a potential candidate for the treatment of ovarian cancer.

#### Appendix. Supplementary data.

The  $^1\text{H}$  NMR and  $^{13}\text{C}$  NMR spectrum of target compounds; the stability of  $^1\text{H}$  NMR spectrum for **2b** in deuterioxide, GSH and NAC; crystallographic information of **2b** and **2l**.

#### Acknowledgments

We thank the financial supports of the National Natural Science Foundation of China (No.81703337), the Priority Academic Program Development of Jiangsu Higher Education Institutions (Integration of Chinese and Western Medicine), the Jiangsu Specially-Appointed

Professors program, the Six Talent Peaks Project in Jiangsu Province of China (No. SWYY-069), the Open Project of Chinese Materia Medica First-Class Discipline of Nanjing University of Chinese Medicine (No. 2020YLXK010), and Postgraduate Research & Practice Innovation Program of Jiangsu Province (No. KYCX20\_1564, KYCX20\_1510, SJCX20\_0532). We also thank for the experimental support from the experiment center for science and technology, Nanjing University of Chinese Medicine.

## References

- An, B., Wang, B., Hu, J., Xu, S., Huang, L., Li, X., & Chan, A. S. C. (2018). Synthesis and biological evaluation of selenium-containing 4-anilinoquinazoline derivatives as novel antimitotic agents. *J. Med. Chem.*, *61*, 2571-2588. doi:10.1021/acs.jmedchem.8b00128
- An, B., Zhang, S., Hu, J., Pan, T., Huang, L., Tang, J. C., Chan, A. S. C. (2018). The design, synthesis and evaluation of selenium-containing 4-anilinoquinazoline hybrids as anticancer agents and a study of their mechanism. *Org. Biomol. Chem.*, *16*, 4701-4714. doi:10.1039/c8ob00875b
- Banerjee, S., & Kaye, S. B. (2013). New strategies in the treatment of ovarian cancer: current clinical perspectives and future potential. *Clin. Cancer Res.*, *19*(5), 961-968. doi:10.1158/1078-0432.CCR-12-2243
- Bian, M., Fan, R., Jiang, G., Wang, Y., Lu, Y., & Liu, W. (2020). Halo and pseudohalo gold(I)-NHC complexes derived from 4,5-diarylimidazoles with excellent in vitro and in vivo anticancer activities against HCC. *J. Med. Chem.*, *63*, 9197-9211. doi:10.1021/acs.jmedchem.0c00257
- Bian, M., Fan, R., Zhao, S., & Liu, W. (2019). Targeting the thioredoxin system as a strategy for cancer therapy. *J. Med. Chem.*, *62*, 7309-7321. doi:10.1021/acs.jmedchem.8b01595
- Cairns, R. A., Harris, I. S., & Mak, T. W. (2011). Regulation of cancer cell metabolism. *Nat. Rev. Cancer*, *11*, 85-95. doi:10.1038/nrc2981
- Casini, A., Sun, R. W., & Ott, I. (2018). Medicinal chemistry of gold anticancer metallodrugs. *Met. Ions Life Sci.*, *18*, 199-217. doi:10.1515/9783110470734-013

- Deng, Z., Yu, L., Cao, W., Zheng, W., & Chen, T. (2015). A selenium-containing ruthenium complex as a cancer radiosensitizer, rational design and the important role of ROS-mediated signalling. *Chem. Commun.*, 51, 2637-2640. doi:10.1039/c4cc07926d
- Dharmaraja, A. T. (2017). Role of reactive oxygen species (ROS) in therapeutics and drug resistance in cancer and bacteria. *J. Med. Chem.*, 60, 3221-3240. doi:10.1021/acs.jmedchem.6b01243
- Dos Santos, D. C., Rafique, J., Saba, S., Almeida, G. M., Siminski, T., Padua, C., . . . Ourique, F. (2020). Apoptosis oxidative damage-mediated and antiproliferative effect of selenylated imidazo[1,2-a]pyridines on hepatocellular carcinoma HepG2 cells and in vivo. *J. Biochem. Mol. Toxic.*, e22663-e22663. doi:10.1002/jbt.22663
- Engman, L., Cotgreave, I., Angulo, M., Taylor, C. W., Paine-Murrieta, G. D., & Powis, G. (1997). Diaryl chalcogenides as selective inhibitors of thioredoxin reductase and potential antitumor agents. *Anticancer Res.*, 17, 4599-4605.
- Fan, R., Bian, M., Hu, L., & Liu, W. (2019). A new rhodium(I) NHC complex inhibits TrxR: In vitro cytotoxicity and in vivo hepatocellular carcinoma suppression. *Eur. J. Med. Chem.*, 183, 111721-111721. doi:10.1016/j.ejmech.2019.111721
- Fernandes, A. P., & Gandin, V. (2015). Selenium compounds as therapeutic agents in cancer. *Biochimica Et Biophysica Acta-General Subjects*, 1850, 1642-1660. doi:10.1016/j.bbagen.2014.10.008
- Gandin, V., Khalkar, P., Braude, J., & Fernandes, A. P. (2018). Organic selenium compounds as potential chemotherapeutic agents for improved cancer treatment. *Free Radical Bio. Med.*, 127, 80-97. doi:10.1016/j.freeradbiomed.2018.05.001
- Garcia-Garcia, P., Martinez, A., Sanjuan, A. M., Fernandez-Rodriguez, M. A., & Sanz, R. (2011). Gold(I)-catalyzed tandem cyclization-selective migration reaction of 1,3-dien-5-yne: regioselective synthesis of highly substituted benzenes. *Org. Lett.*, 13, 4970-4973. doi:10.1021/ol202129n
- Gautier, A., & Cisnetti, F. (2012). Advances in metal-carbene complexes as potent anti-cancer agents. *Metallomics*, 4, 23-32. doi:10.1039/c1mt00123j

- Gorrini, C., Harris, I. S., & Mak, T. W. (2013). Modulation of oxidative stress as an anticancer strategy. *Nat. Rev. Drug Discov.*, *12*, 931-947. doi:10.1038/nrd4002
- Gothe, Y., Marzo, T., Messori, L., & Metzler-Nolte, N. (2015). Cytotoxic activity and protein binding through an unusual oxidative mechanism by an iridium(I)-NHC complex. *Chem. Commun.*, *51*(15), 3151-3153. doi:10.1039/c4cc10014j
- Harlepp, S., Chardon, E., Bouche, M., Dahm, G., Maaloum, M., & Bellemin-Laponnaz, S. (2019). N-heterocyclic carbene-platinum complexes featuring an anthracenyl moiety: anti-cancer activity and DNA interaction. *Int. J. Mol. Sci.*, *20*(17). doi:10.3390/ijms20174198
- He, L., Ji, S., Lai, H., & Chen, T. (2015). Selenadiazole derivatives as theranostic agents for simultaneous cancer chemo-/radiotherapy by targeting thioredoxin reductase. *J. Mater. Chem. B*, *3*, 8383-8393. doi:10.1039/c5tb01501d
- Hickey, J. L., Ruhayel, R. A., Barnard, P. J., Baker, M. V., Berners-Price, S. J., & Filipovska, A. (2008). Mitochondria-targeted chemotherapeutics: the rational design of gold(I) N-heterocyclic carbene complexes that are selectively toxic to cancer cells and target protein selenols in preference to thiols. *J. Am. Chem. Soc.*, *130*, 12570-12571. doi:10.1021/ja804027j
- Hosnedlova, B., Kepinska, M., Skalickova, S., Fernandez, C., Ruttkay-Nedecky, B., Malevu, T. D., Kizek, R. (2017). A summary of new findings on the biological effects of selenium in selected animal species-a critical review. *Int. J. Mol. Sci.*, *18*, 2209-2209. doi:10.3390/ijms18102209
- Huang, K. B., Wang, F. Y., Tang, X. M., Feng, H. W., Chen, Z. F., Liu, Y. C., Liang, H. (2018). Organometallic gold(III) complexes similar to tetrahydroisoquinoline induce ER-stress-mediated apoptosis and pro-death autophagy in A549 cancer cells. *J. Med. Chem.*, *61*, 3478-3490. doi:10.1021/acs.jmedchem.7b01694
- Ibrahim, S. A. Z., Kerkadi, A., & Agouni, A. (2019). Selenium and health: an update on the situation in the middle east and north africa. *Nutrients*, *11*, 1457-1457. doi:10.3390/nu11071457
- Ip, C., Lisk, D. J., & Ganther, H. E. (1998). Activities of structurally-related lipophilic selenium

---

compounds as cancer chemopreventive agents. *Anticancer Res.*, 18, 4019-4025.

Kala, S., Mak, A. S., Liu, X., Posocco, P., Pricl, S., Peng, L., & Wong, A. S. (2014). Combination of dendrimer-nanovector-mediated small interfering RNA delivery to target Akt with the clinical anticancer drug paclitaxel for effective and potent anticancer activity in treating ovarian cancer. *J. Med. Chem.*, 57(6), 2634-2642. doi:10.1021/jm401907z

Kamal, A., Nazari, V. M., Yaseen, M., Iqbal, M. A., Ahamed, M. B. K., Majid, A. S. A., & Bhatti, H. N. (2019). Green synthesis of selenium-N-heterocyclic carbene compounds: evaluation of antimicrobial and anticancer potential. *Bioorg. Chem.*, 90, 103042-103042. doi:10.1016/j.bioorg.2019.103042

Khalkar, P., Ali, H. A., Codo, P., Argelich, N. D., Martikainen, A., Arzenani, M. K., Fernandes, A. P. (2018). Selenite and methylseleninic acid epigenetically affects distinct gene sets in myeloid leukemia: A genome wide epigenetic analysis. *Free Radical Biol. Med.*, 117, 247-257. doi:10.1016/j.freeradbiomed.2018.02.014

Lai, H., Fu, X., Sang, C., Hou, L., Feng, P., Li, X., & Chen, T. (2018). Selenadiazole derivatives inhibit angiogenesis-mediated human breast tumor growth by suppressing the VEGFR2-Mediated ERK and AKT signaling pathways. *Chem. Asian. J.*, 13, 1447-1457. doi:10.1002/asia.201800110

Li, Y., Tan, C. P., Zhang, W., He, L., Ji, L. N., & Mao, Z. W. (2015). Phosphorescent iridium(III)-bis-N-heterocyclic carbene complexes as mitochondria-targeted theranostic and photodynamic anticancer agents. *Biomaterials*, 39, 95-104. doi:10.1016/j.biomaterials.2014.10.070

Li, Z., Carrier, L., Belame, A., Thiyagarajah, A., Salvo, V. A., Burow, M. E., & Rowan, B. G. (2009). Combination of methylselenocysteine with tamoxifen inhibits MCF-7 breast cancer xenografts in nude mice through elevated apoptosis and reduced angiogenesis. *Breast Cancer Res. Tr.*, 118, 33-43. doi:10.1007/s10549-008-0216-x

Liang, Y., Zhou, Y., Deng, S., & Chen, T. (2016). Microwave-assisted syntheses of benzimidazole-containing selenadiazole derivatives that induce cell-cycle arrest and apoptosis in human breast cancer cells by activation of the ROS/AKT pathway.

- Liang, Y. W., Zheng, J. S., Li, X. L., Zheng, W. J., & Chen, T. F. (2014). Selenadiazole derivatives as potent thioredoxin reductase inhibitors that enhance the radiosensitivity of cancer cells. *Eur. J. Med. Chem.*, 84, 335-342. doi:10.1016/j.ejmech.2014.07.032
- Liu, W., Bendorf, K., Hagenbach, A., Abram, U., Niu, B., Mariappan, A., & Gust, R. (2011). Synthesis and biological studies of silver N-heterocyclic carbene complexes derived from 4,5-diarylimidazole. *Eur. J. Med. Chem.*, 46, 5927-5934. doi:10.1016/j.ejmech.2011.10.002
- Liu, W., Bendorf, K., & Proetto, M. (2011). NHC gold halide complexes derived from 4,5-diarylimidazoles: synthesis, structural analysis, and pharmacological investigations as potential antitumor agents *J. Med. Chem.*, 54, 8605-8615. doi:10.1021/jm201156x
- Liu, W., Bendorf, K., & Proetto, M. (2012). Synthesis, characterization, and in vitro studies of bis[1,3-diethyl-4,5-diarylimidazol-2-ylidene]gold(I/III) complexes. *J. Med. Chem.*, 55, 3713-3724. doi:10.1021/jm3000196
- Liu, W., & Gust, R. (2013). Metal N-heterocyclic carbene complexes as potential antitumor metallodrugs. *Chem. Soc. Rev.*, 42, 755-773. doi:10.1039/c2cs35314h
- Long, Y., Cao, B., Xiong, X., Chan, A. S. C., Sun, R. W., & Zou, T. (2020). Bioorthogonal activation of dual catalytic and anti-cancer activities of organogold(I) complexes in living systems. *Angew Chem. Int. Ed.*, 60(68):4133-4141. doi:10.1002/anie.202013366
- Lu, M. C., Jiao, Q., Liu, T., Tan, S. J., Zhou, H. S., You, Q. D., & Jiang, Z. Y. (2018). Discovery of a head-to-tail cyclic peptide as the Keap1-Nrf2 protein-protein interaction inhibitor with high cell potency. *Eur. J. Med. Chem.*, 143, 1578-1589. doi:10.1016/j.ejmech.2017.10.052
- Mercs, L., & Albrecht, M. (2010). Beyond catalysis: N-heterocyclic carbene complexes as components for medicinal, luminescent, and functional materials applications. *Chem. Soc. Rev.*, 39, 1903-1912. doi:10.1039/b902238b
- Meyer, A., Oehninger, L., Geldmacher, Y., Alborzina, H., Wolf, S., Sheldrick, W. S., & Ott, I. (2014). Gold(I) N-heterocyclic carbene complexes with naphthalimide ligands as combined thioredoxin reductase inhibitors and DNA intercalators. *ChemMedChem*, 9, 1794-1800.

---

doi:10.1002/cmdc.201402049

Misra, S., Boylan, M., Selvam, A., Spallholz, J. E., & Bjornstedt, M. (2015). Redox-active selenium compounds--from toxicity and cell death to cancer treatment. *Nutrients*, *7*, 3536-3556.

doi:10.3390/nu7053536

Nelson, D. J., Nahra, F., Patrick, S. R., Cordes, D. B., Slawin, A. M. Z., & Nolan, S. P. (2014). Exploring the coordination of cyclic selenoureas to gold(I). *Organometallics*, *33*, 3640-3645. doi:10.1021/om500610w

Nguyen, N., Sharma, A., Nguyen, N., Sharma, A. K., Desai, D., Huh, S. J., Robertson, G. P. (2011). Melanoma chemoprevention in skin reconstructs and mouse xenografts using isoselenocyanate-4. *Cancer Prev. Res.*, *4*, 248-258. doi:10.1158/1940-6207.CAPR-10-0106

Pelicano, H., Carney, D., & Huang, P. (2004). ROS stress in cancer cells and therapeutic implications. *Drug Resist. Update*, *7*, 97-110. doi:10.1016/j.drug.2004.01.004

Reich, H. J., & Hondal, R. J. (2016). Why nature chose selenium. *ACS. Chem. Biol.*, *11*, 821-841. doi:10.1021/acscchembio.6b00031

Rothmund, M., Bar, S. I., Rehm, T., Kostrhunova, H., Brabec, V., & Schobert, R. (2020). Antitumoral effects of mitochondria-targeting neutral and cationic cis-[bis(1,3-dibenzylimidazol-2-ylidene)Cl(L)]Pt(II) complexes. *Dalton Trans.*, *49*(26), 8901-8910. doi:10.1039/d0dt01664k

Saleh, A. M., Aljada, A., El-Abadelah, M. M., Sabri, S. S., Zahra, J. A., Nasr, A., & Aziz, M. A. (2015). The pyridone-annelated isoindigo (5'-Cl) induces apoptosis, dysregulation of mitochondria and formation of ROS in leukemic HL-60 cells. *Cell Physiol. Biochem.*, *35*, 1958-1974. doi:10.1159/000374004

Sanmartin, C., Plano, D., & Palop, J. A. (2008). Selenium compounds and apoptotic modulation: a new perspective in cancer therapy. *Mini-Rev. Med. Chem.*, *8*, 1020-1031. doi:10.2174/138955708785740625

Selenius, M., Hedman, M., Brodin, D., Gandin, V., Rigobello, M. P., Flygare, J., Fernandes, A. P. (2012). Effects of redox modulation by inhibition of thioredoxin reductase on

radiosensitivity and gene expression. *J. Cell Mol. Med.*, *16*, 1593-1605. doi:10.1111/j.1582-4934.2011.01469.x

Seliman, A. A. A., Altaf, M., Odewunmi, N. A., Kawde, A. N., Zierkiewicz, W., Ahmad, S., Isab, A. A. (2017). Synthesis, X-ray structure, DFT calculations and anticancer activity of a selenourea coordinated gold(I)-carbene complex. *Polyhedron*, *137*, 197-206. doi:10.1016/j.poly.2017.08.003

Siegel, R., Naishadham, D., & Jemal, A. (2013). Cancer statistics, 2013. *CA Cancer J. Clin.*, *63*(1), 11-30. doi:10.3322/caac.21166

Sze, J. H., Ranninga, P. V., Nakamura, K., Casey, M., Khanna, K. K., Berners-Price, S. J., Tonissen, K. F. (2020). Anticancer activity of a Gold(I) phosphine thioredoxin reductase inhibitor in multiple myeloma. *Redox Biol.*, *28*, 101310-101310. doi:10.1016/j.redox.2019.101310

Teyssot, M. L., Jarrousse, A. S., Manin, M., Chevy, A., Roche, S., Norre, F., Gautier, A. (2009). Metal-NHC complexes: a survey of anti-cancer properties. *Dalton Trans.*, 6894-6902. doi:10.1039/b906308k

Tham, M. J. R., Babak, M. V., & Ang, W. H. (2020). PlatinER: a highly potent anticancer platinum(II) complex that induces endoplasmic reticulum stress driven immunogenic cell death. *Angew Chem. Int. Ed. Engl.*, *59*(43), 19070-19078. doi:10.1002/anie.202008604

Wang, L., Yang, Z., Fu, J., Yin, H., Xiong, K., Tan, Q., Zeng, H. (2012). Ethaselen: a potent mammalian thioredoxin reductase 1 inhibitor and novel organoselenium anticancer agent. *Free Radical Biol. Med.*, *52*, 898-908. doi:10.1016/j.freeradbiomed.2011.11.034

Weiss, R., Reichel, S., Handke, M., & Hampel, F. (1998). Generation and trapping reactions of a formal 1:1 complex between singlet carbon and 2,2'-bipyridine. *Angew. Chem. Int. Ed.*, *37*, 344-347. doi:10.1002/(SICI)1521-3773(19980216)37:3<344::AID-ANIE344>3.0.CO;2-H

Yang, C., Mehmood, F., Lam, T. L., Chan, S. L., Wu, Y., Yeung, C. S., . . . Che, C. M. (2016). Stable luminescent iridium(III) complexes with bis(N-heterocyclic carbene) ligands: photo-stability, excited state properties, visible-light-driven radical cyclization and CO<sub>2</sub> reduction, and cellular imaging. *Chem Sci*, *7*(5), 3123-3136. doi:10.1039/c5sc04458h

Yang, Y., Deng, S., Zeng, Q., Hu, W., & Chen, T. (2016). Highly stable selenadiazole derivatives induce bladder cancer cell apoptosis and inhibit cell migration and invasion through the activation of ROS-mediated signaling pathways. *Dalton Trans.*, 45, 18465-18475. doi:10.1039/c6dt02045c

Yang, Y., Huang, F., Ren, Y., Xing, L., Wu, Y., Li, Z., Xu, C. (2009). The anticancer effects of sodium selenite and selenomethionine on human colorectal carcinoma cell lines in nude mice. *Oncol. Res.*, 18, 1-8. doi:10.3727/096504009789745647

Zeng, D., Deng, S., Sang, C., Zhao, J., & Chen, T. (2018). Rational design of cancer-targeted selenadiazole derivative as efficient radiosensitizer for precise cancer therapy. *Bioconjug. Chem.*, 29, 2039-2049. doi:10.1021/acs.bioconjchem.8b00247

Zhang, J., Li, X., Han, X., Liu, R., & Fang, J. (2017). Targeting the thioredoxin system for cancer therapy. *Trends Pharmacol. Sci.*, 38, 794-808. doi:10.1016/j.tips.2017.06.001

Zhao, J., Zeng, D., Liu, Y., Luo, Y., Ji, S., Li, X., & Chen, T. (2017). Selenadiazole derivatives antagonize hyperglycemia-induced drug resistance in breast cancer cells by activation of AMPK pathways. *Metallomics*, 9, 535-545. doi:10.1039/c7mt00001d

Zou, T., Lum, C. T., Chui, S. S., & Che, C. M. (2013). Gold(III) complexes containing N-heterocyclic carbene ligands: thiol "switch-on" fluorescent probes and anti-cancer agents. *Angew. Chem. Int. Ed.*, 52, 2930-2933. doi:10.1002/anie.201209787